

Code Verification

Table of Contents

Introduction	1
Problem 1 – Three-Dimensional Flow to a Partially-Penetrating Well	1
Problem 2 – Three-Dimensional Solute Transport in a Uniform Flow Field	3
Problem 3 – Depth-Averaged Radial Transport during Injection/Extraction Cycles	6
Problem 4 – Comparison of <i>Adaptive Groundwater</i> and MT3D Numerical Accuracy: 3D Transport of Large-Scale, Highly-Stratified Plumes	8

Introduction

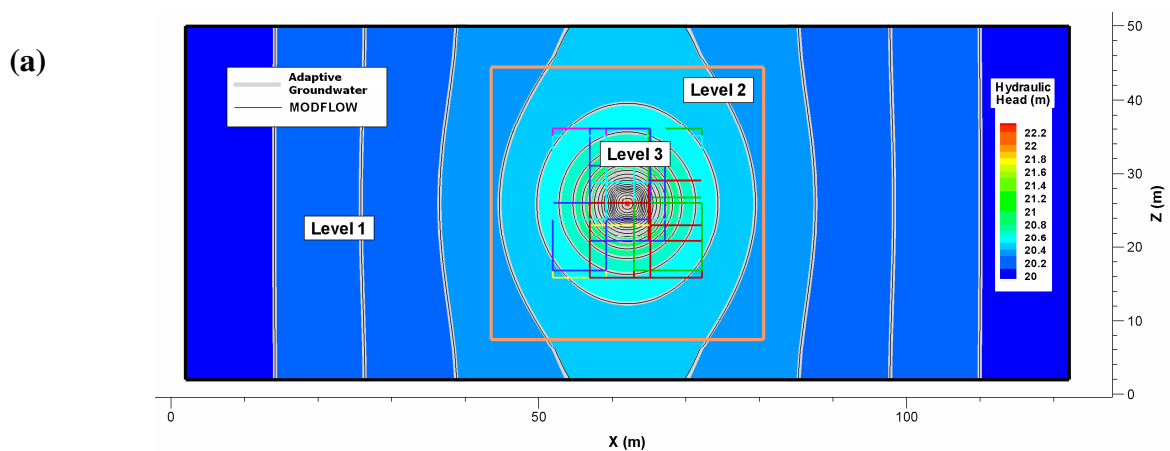
The *Adaptive Groundwater* code is used to analyze test problems involving constant-density, three-dimensional flow and solute transport and radial transport from and toward an injection/extraction well. Simulation results are compared to hydraulic heads and solute concentrations from MODFLOW (McDonald and Harbaugh, 1988), MT3DMS (Zheng, 2000), and analytical solutions. References for this section are presented in the bibliography for the *Adaptive Groundwater* help system.

Three-Dimensional Flow to a Partially-Penetrating Well

The first validation simulation is a steady-state, three-dimensional constant-density drawdown analysis, as shown in Figure 3.10. The confined aquifer is 124 m long, 52 m wide,

and 52 m thick with a hydraulic conductivity equal to 49 m/day. Constant-head boundary conditions (20 m) are maintained at both ends of the flow domain, and no-flow boundary conditions are specified at the top and bottom and y-direction ends of the aquifer. The injection rate is 2,180 m³/day from a partially-penetrating well screened from $z=24$ to 28 m. The horizontal spacing in the MODFLOW mesh gradually increases from 0.25 m near the well to a maximum of 4 m. The vertical spacing varies from 0.25 m near the well screen to 1 m in the vicinity of the aquifer boundaries. The *Adaptive Groundwater* mesh consists of three levels of refinement [Figure 3.10(a)]. The base grid contains 4 m cubic cells and the refinement factor is four (i.e., 25 cm mesh spacing on Level 3).

Figures 3.10(a,b) are vertical (x - z) cross-sections through the center of the injection well. The agreement between the steady-state hydraulic head distributions computed using the two codes is excellent. The same-level and coarse-fine subgrid pressure boundary condition techniques outlined above produce smooth hydraulic-head transitions from one subgrid to another.



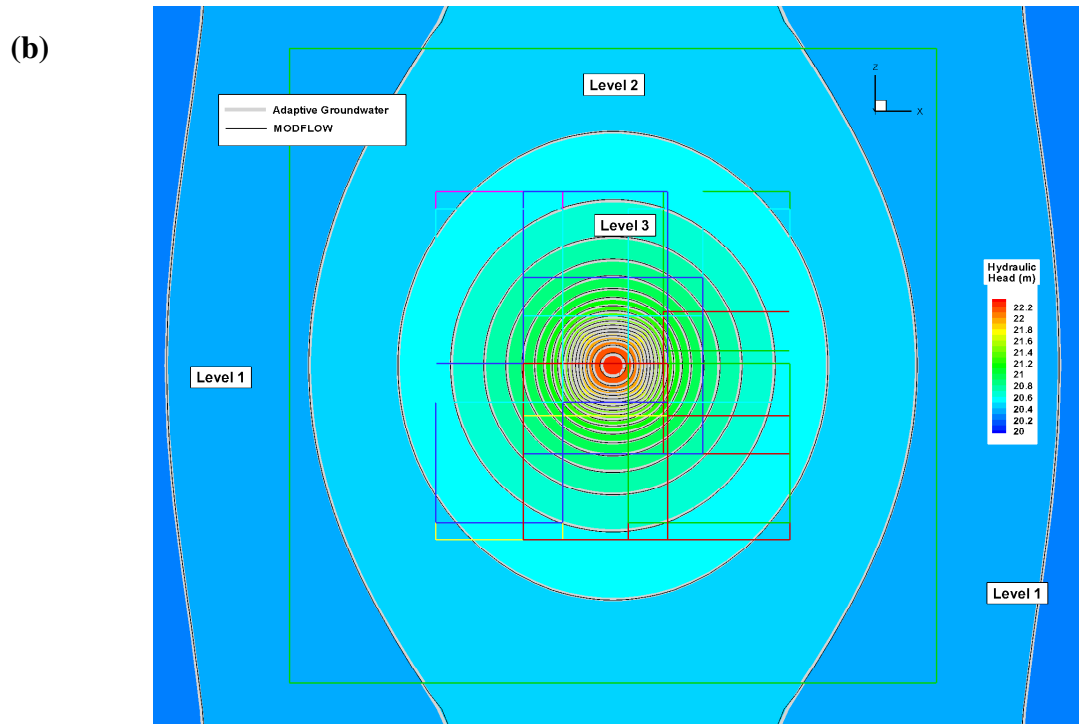


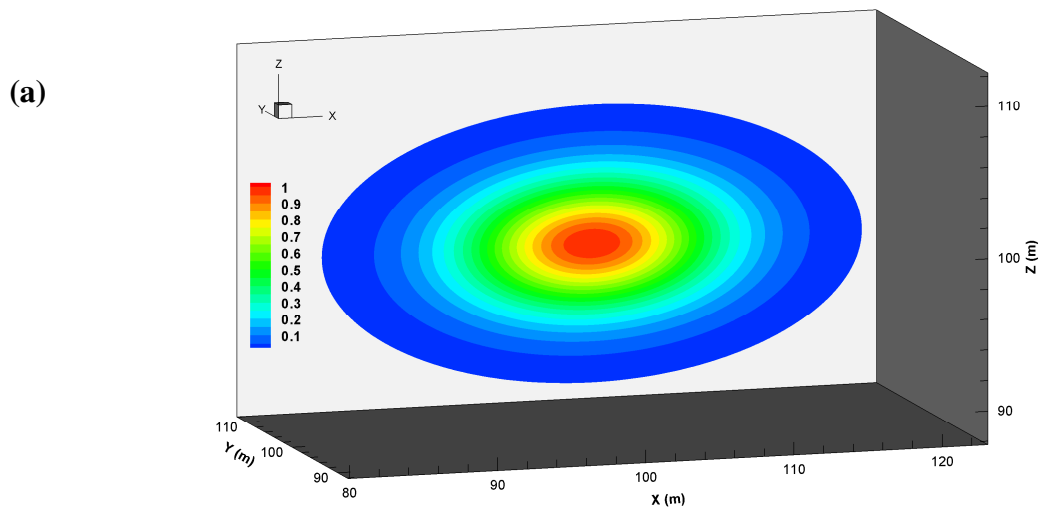
Figure 3.10
Adaptive Groundwater Code Verification
Three-Dimensional, Steady-State Constant-Density Flow
Hydraulic Head during Injection from a Partially-Penetrating Well
Vertical Cross-Sections: (a) Regional View; (b) Close-up

Three-Dimensional Solute Transport in a Uniform Flow Field

The second test problem is a simulation of three-dimensional, constant-density advection-dispersion in a uniform flow field. The analytical solution for an instantaneous point source in a uniform velocity field (Domenico and Schwartz, 1998) describes the temporal development of a Gaussian concentration distribution with different longitudinal and transverse standard deviations (i.e., length scales). In this simulation, the x -direction velocity is equal to 1.0 m/day and the longitudinal and transverse (y - and z -directions) dispersivities are equal to 10 and 2.5 cm,

respectively. The starting plume for the *Adaptive Groundwater* simulation is based on the analytical solution for $t=180$ days and a maximum plume concentration of 1.0 [Figure 3.11(a)]. The simulated $c=0.1$ isosurface and the Level 3 subgrid boundaries after 100 days of transport are shown in Figure 3.11(b). The Levels 1, 2, and 3 cell dimensions are 4, 1, and 0.25 m, respectively, in the AMR mesh.

Figure 3.11(c) compares the simulated and analytical solute distributions after 100 days of transport in the aquifer. The Level 3 AMR grid consists of 16 subgrids at the end of the simulation. The maximum solute concentration in the plume is plotted versus time in Figure 3.11(d). The agreement between the simulated and exact concentration distributions is excellent. For example, the difference between the simulated and exact maximum plume concentrations after 100 days is about 0.001.



(b)

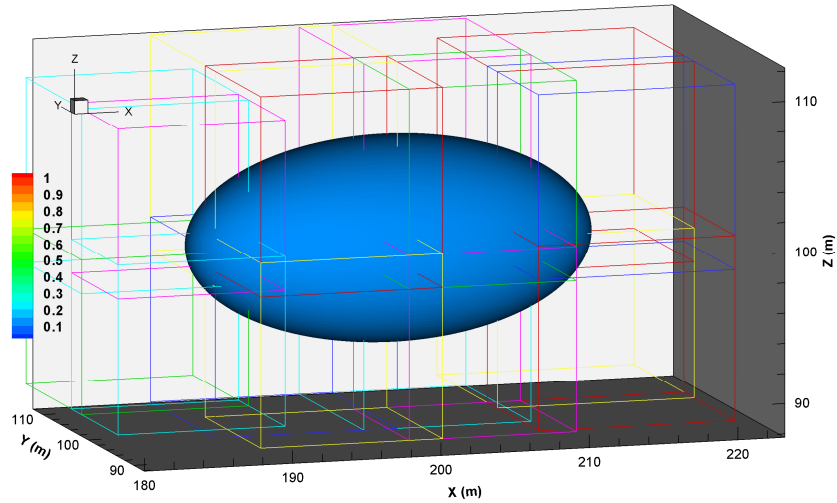


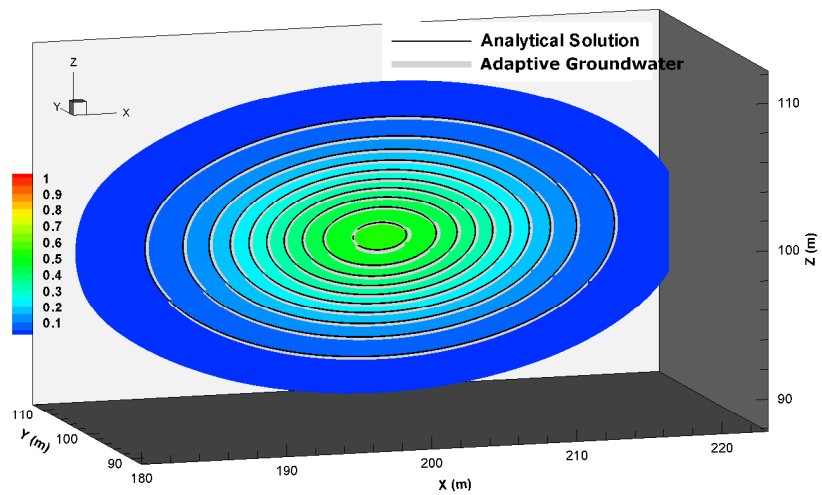
Figure 3.11

***Adaptive Groundwater* Code Verification**

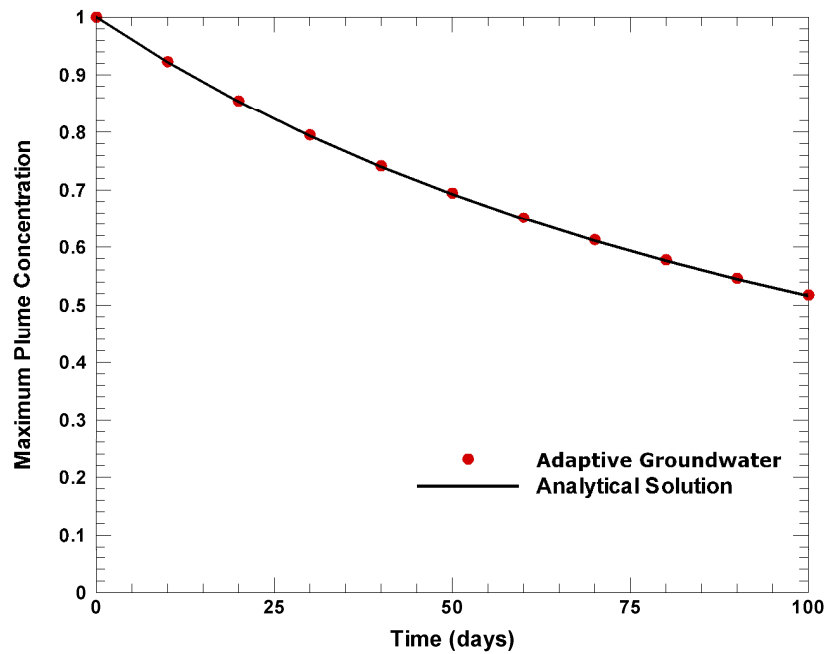
Three-Dimensional, Constant-Density Solute Transport

- (a) x - z Cross-Section Showing Initial ($t=0$) Solute Distribution
- (b) $c=0.1$ Isosurface and Level 3 Subgrid Boundaries at $t=100$ days
- (c) x - z Slice with Simulated and Exact Solute Distributions at $t=100$ days
- (d) Maximum Plume Concentration vs. Time

(c)



(d)



Depth-Averaged Radial Transport during Injection/Extraction Cycles

Gelhar and Collins (1971) derived an approximate analytical solution for the solute concentration at a fully-penetrating pumping well during an injection/extraction cycle in a confined aquifer. Zheng and Wang (1998) present the simulation results for MT3DMS simulations of this radial advection-dispersion problem using three transport equation solution algorithms: ULTIMATE, MMOC, and upstream finite difference. Solute with a concentration equal to C_0 was injected at a rate of $2,450 \text{ m}^3/\text{day}$ for 2.5 years, and the resulting plume was extracted at the same rate for a period of 7.5 years. The flow field was assumed to reach equilibrium instantaneously for both pumping rates. Zheng and Wang (1998) summarize the other transport parameter values. The MT3DMS grid contained one layer and square plan-view cells with sides of 274 m. *Adaptive Groundwater* was also used to simulate this problem using

the same input parameters and an AMR mesh containing four levels of refinement and the following horizontal, square cell dimensions: 1,096 m (Base Grid); 548 m (Level 2); 274 m (Level 3); and 137 m (Level 4). The Level 4 AMR cells were two times smaller than the MT3DMS cells in order to improve the mass balance (i.e., ensure that the correct solute mass was injected into the aquifer).

The simulated solute concentrations at the pumping well for both codes are compared with the analytical solution in Figure 3.12. The *Adaptive Groundwater*, MMOC, and ULTIMATE simulations are generally in good agreement with the analytical solution. However, the upstream finite difference solution is much less accurate due to numerical dispersion. A plume animation (movie file) for this problem, including pore velocity vectors and AMR mesh at different times during the injection/extraction cycles, is presented in the *Adaptive Groundwater* help documentation.

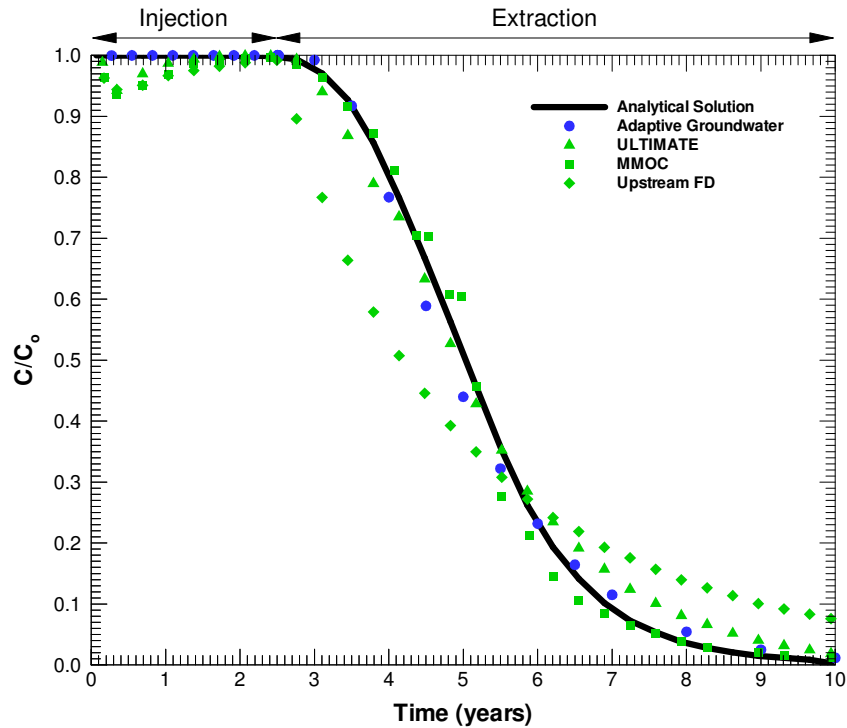


Figure 3.12
Adaptive Groundwater Code Verification
Radial Transport during Pumping Well Injection/Extraction Cycles
Concentration vs. Time at the Well

Three-Dimensional Advection and Dispersion of Field-Scale Plumes with Large Vertical Concentration Gradients

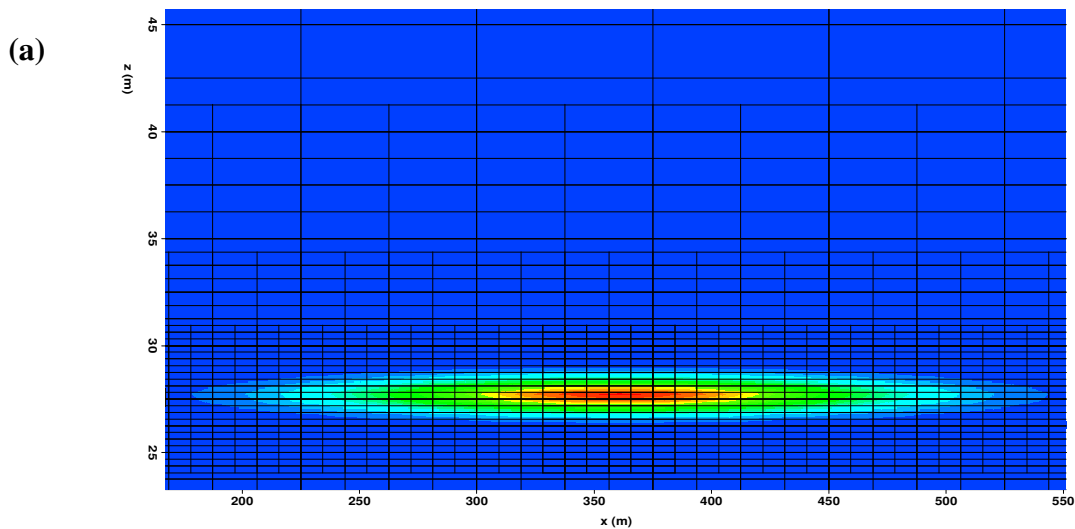
This fourth test problem analyzes three-dimensional, constant-density transport of field-scale contaminant plumes characterized by large vertical concentration gradients and small vertical dispersion. The objective of this problem is to illustrate the importance of the following factors in simulations of such plumes: (i) the reduction of artificial numerical dispersion based on the implementation of a highly-accurate numerical solution of the solute advection term in the transport equation; (ii) the ability of the numerical scheme to handle small dispersivities (e.g.,

vertical direction) without introducing spurious oscillations into the computed concentration distribution (i.e., handle large Peclet numbers); (iii) the capability of the numerical code to reduce the total number of cells in the grid by minimizing unnecessary discretization (e.g., excessively fine vertical cell thicknesses to satisfy accuracy and stability constraints) and adapting the high-level mesh refinement to the transient position of the plume; and (iv) the capability of the code to use large time steps (Δt) that are determined by accuracy requirements (e.g., resolving a pumping well effluent curve) rather than by Courant stability limitations. As shown below, factor (iii) is closely related to the others.

The analytical solution for an instantaneous point source in a uniform velocity field (Domenico and Schwartz, 1998; Equation 18.24) defines the maximum concentration at the centroid of a Gaussian plume in a uniform flow field. Three different Gaussian plumes were simulated using *Adaptive Groundwater* and MT3DMS (Zheng, 2000) using Visual MODFLOW version 2.8.2. For the MT3DMS runs two of the advection solutions were examined: MMOC and ULTIMATE. The MMOC (modified method of characteristics) option is basically a semi-Lagrangian scheme that uses a lower-order (linear) interpolation polynomial to compute concentrations at the feet of the characteristics. The ULTIMATE algorithm (Universal Limiter for Transient Interpolation Modeling of the Advective Transport Equations) is a higher-order solution that utilizes cubic polynomials for concentration interpolation and a universal flux limiter to control unphysical oscillations.

Vertical slice plots of the starting concentration distribution for the two plumes that were analyzed are shown in Figures 3.13a (thinner plume) and 3.13b (2x thicker). The plume concentration varies from 0.0 to 1.0. For a Gaussian plume most of the contaminant mass is contained within a distance of +/- three standard deviations (σ) from the centroid. Accordingly,

the size of the thinner plume is characterized by $\sigma_L = 450$ m, $\sigma_{TH} = 150$ m, $\sigma_{TV} = 3.0$ m in the x -, y -, and z -directions, respectively. The thicker plume has the same horizontal dimensions but twice the vertical dimension ($\sigma_{TV} = 6.0$ m). The local AMR mesh for *Adaptive Groundwater* with five levels of refinement (cell refinement factor equal to 2) is also shown. The dimensions of the Level 5 cells were: $\Delta_x = \Delta_y = 9.375$ m and $\Delta_z = 0.3125$ m. The MT3DMS grid used the same Level 5 cell sizes within the plume area for the entire simulation time. Three different simulations were performed with both codes using different longitudinal (α_L), transverse horizontal (α_{TH}), and transverse vertical (α_{TV}) dispersivities: (1) thicker plume/ “medium” dispersion ($\alpha_L = 2.5$ m, $\alpha_{TH} = 0.28$ m, $\alpha_{TV} = 4.4E-4$ m); (2) thin plume/larger dispersion ($\alpha_L = 10$ m, $\alpha_{TH} = 1.1$ m, $\alpha_{TV} = 4.4E-4$ m); and (3) thin plume/small dispersion ($\alpha_L = 0.1$ m, $\alpha_{TH} = 0.011$ m, $\alpha_{TV} = 4.4E-6$ m). The uniform groundwater pore velocity (V_x) in all cases was 11.7 m/yr.



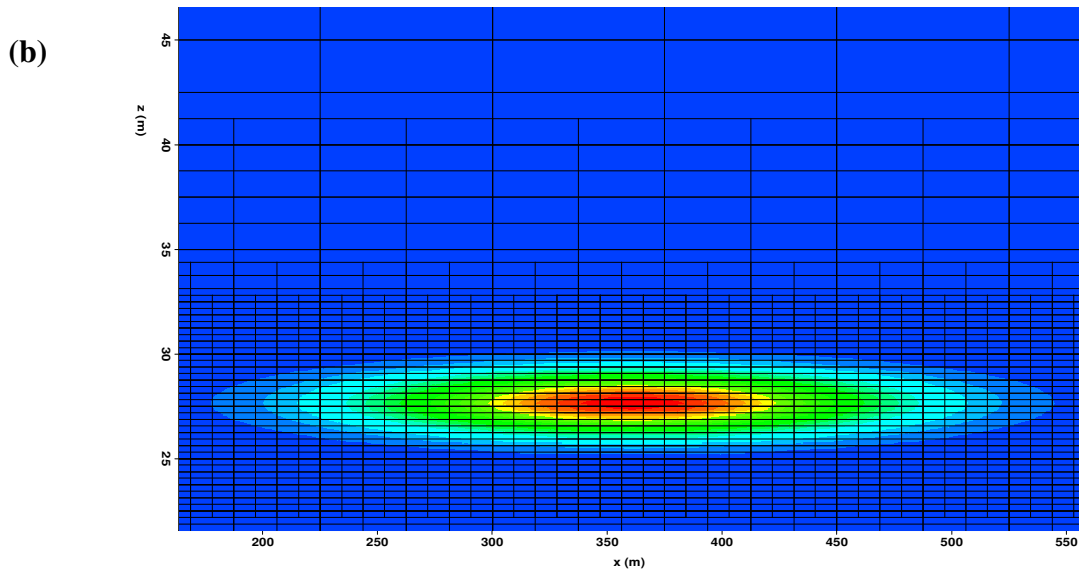
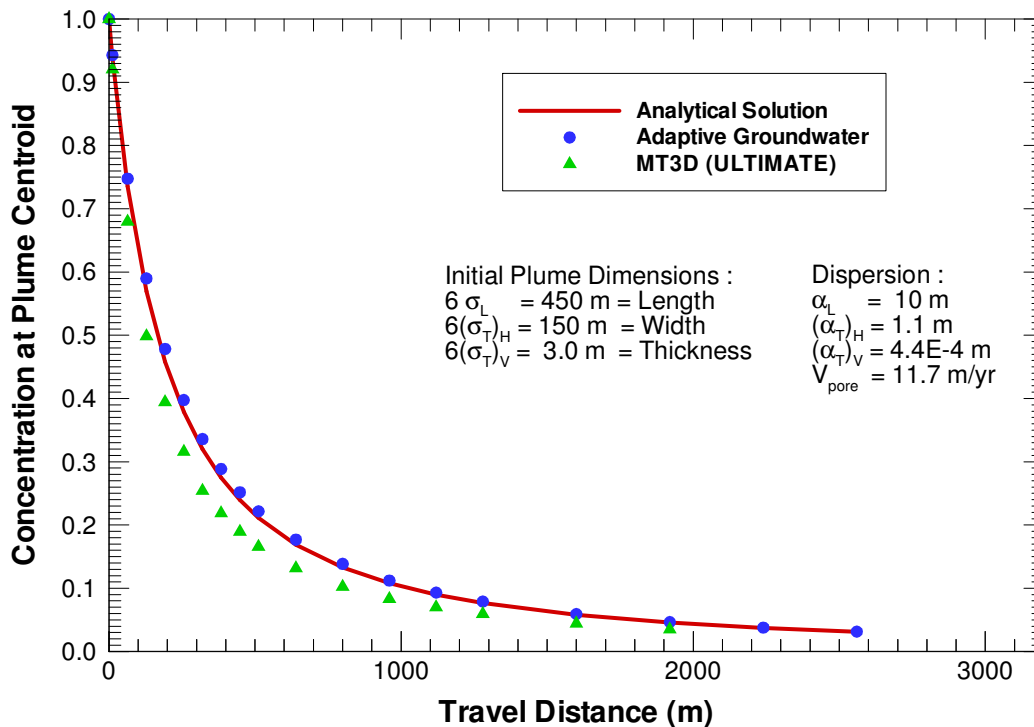


Figure 3.13
***Adaptive Groundwater* Code Verification**
Three-Dimensional, Field-Scale Plume Transport
x-z Sections through Initial Gaussian Concentration Distribution (c=0-1)
(a) Thinner Plume; (b) Thicker Plume

Graphs of the simulated maximum (centroid) plume concentrations versus time [$C_{max}(t)$] for these three cases are presented in Figures 3.14 a-c. Movies of plume animations for the *Adaptive Groundwater* simulations are presented in the program help documentation. As shown in the $C_{max}(t)$ graphs, the *Adaptive Groundwater* results (5th-order interpolation polynomials) agree almost exactly with the analytical solution in all cases throughout the simulation period. In contrast, both of the MT3DMS advection algorithms underpredict the exact concentrations due to numerical dispersion. The MMOC results exhibit significant numerical dispersion, which is consistent with the implementation of linear interpolation polynomials in semi-Lagrangian methods (Baptista, 1987; Leonard, 2002). For the thinner plume and small dispersion [Figure 3.13 (c)] the ULTIMATE scheme results are almost 50 percent less than the analytical solution and exhibit nonphysical, Peclet-type oscillations. To a lesser degree, the ULTIMATE solution in

(b)



(c)

